

Control of LVRT of PMSG in Back-to-Back Wind Energy Conversion System

Abstract. The paper presents the control scheme of variable speed wind turbine system with direct-driven Permanent Magnet Synchronous Generator (PMSG) during the Low-Voltage Ride-Through (LVRT). The requirements of LVRT are very important to guarantee the stability of the whole wind energy system during voltage dips. To avoid the dangerous states during the voltage sags the kinetic energy storage in inertia of the wind turbine, DC active crowbar and pitch angle controller have been used. The simulation results confirmed the good performance of the proposed control strategy during the unsymmetrical voltage sag.

Streszczenie. W artykule przedstawiono bezprzekładniowy system turbiny wiatrowej o zmiennej prędkości z generatorem PMSG podczas zapadu napięcia sieci. Spełnienie wymagań LVRT podczas spadków napięcia sieci są bardzo ważne i gwarantują stabilność systemu elektrowni wiatrowej. W celu ograniczenia negatywnego wpływu awaryjnego stanu sieci, zastosowano układ pozwalający na wykorzystanie energii kinetycznej zgromadzonej w wirniku turbiny wiatrowej. W celu dodatkowej ochrony systemu elektrowni wiatrowej zastosowano układ z sterownikami impulsowym oraz algorytm sterowania kątem nachyleniem łopat. Badania symulacyjne potwierdziły prawidłowość i dużą dokładność sterowania systemu elektrowni wiatrowej z generatorem PMSG podczas niesymetrycznego zapadu napięcia sieci. (Sterowanie turbiny wiatrowej z generatorem PMSG podczas zapadu napięcia sieci z układem przekształtnikowym typu back-to-back).

Keywords: wind turbine, PMSG, LVRT, simulation studies

Słowa kluczowe: turbina wiatrowa, PMSG, LVRT, badania symulacyjne

Introduction

In recent years the wind energy conversion systems (WECs) are the one of fastest growing energy resources among the other renewable generation technologies. Due to the increased trend of development of the wind energy conversion systems and their influence of the AC grid, the knowledge of behavior of these systems during grid faults is very important and should be exactly considered [1, 2, 3].

Nowadays, the requirements of grid connection of WECs are very trend topics [4]. These requirements describe the behavior of the wind turbine systems and the power flow during the grid fault and disturbance, especially the stability of systems at the Point of Common Coupling (PCC). During the Low-Voltage Ride-Through (LVRT), the power injected to AC grid by the wind turbine system is respectively limited by the voltage reduction. During the voltage dips, the wind energy conversion system with application of conventional control scheme may cause the increase of the DC-link voltage to extremely high value.

According to requirements of LVRT, the wind turbine system should remain connected to the AC grid for specific time period, in order to prevent the adverse influence of this voltage dip [5, 6]. Therefore, the wind energy conversion system should also provide the appropriate reactive power delivering to the AC grid in order to the support of the grid system.

The injection of the reactive current to the grid allows to preserve the connection of the wind energy conversion system to the AC grid. This also allows to recover the system to the previous state. To manage with these grid faults, the special control scheme for wind energy conversion system with PMSG should be applied. The solutions for symmetrical voltage dips can be found in the literature [7].

The objective of this paper is to analyze the behavior of the wind energy conversion system with direct driven PMSG during the unsymmetrical voltage sags. The proposed control strategy manages with kinetic energy storage in rotor inertia of wind turbine and PMSG for requirements of the LVRT.

To enhance the capability of the LVRT of the direct-driven wind energy conversion system with PMSG, the chopper with damping resistor and pitch controller have been applied. Under voltage sags, the electrical power flow between two converters will be unbalanced, so the control system should deals with this dangerous state.

Wind turbine aerodynamic model

The mechanical power produced by wind turbine can be described with the following equation [6, 8]:

$$(1) \quad P_t = 0.5 \rho A C_p (\lambda, \beta) v_w^3$$

where: ρ - air density; $A = \pi R^2$ - area swept by the rotor blades; R - radius of the turbine blades; C_p - power coefficient of the wind turbine; β - blade pitch angle v_w - wind speed; λ - tip speed ratio, which is defined as:

$$(2) \quad \lambda = \omega_m R / v_w$$

where ω_m - the mechanical angular speed of the turbine and PMSG rotor.

The dynamic equation of mechanical motion of wind turbine system is given by:

$$(3) \quad T_t + T_e = J \cdot \frac{d\omega_m}{dt} + B_f \omega_m$$

where: T_t - the mechanical torque of wind turbine; T_e - the electromagnetic torque of generator; J - the total inertia of the system; B_f - coefficient of viscous friction;

Permanent Magnet Synchronous Generator Model

The model of the PMSG was developed in the synchronous rotating rectangular dq reference frame. The equations of the PMSG in this reference frame can be described as follows: [1, 5, 9]:

$$(4) \quad v_{sd} = R_s i_{sd} + L_d \frac{di_{sd}}{dt} - \omega_e \psi_{sq}$$

$$(5) \quad v_{sq} = R_s i_{sq} + L_q \frac{di_{sq}}{dt} + \omega_e \psi_{sd}$$

The components of stator flux vector in this reference frame are given by:

$$(6) \quad \psi_{sd} = L_d i_{sd} + \psi_{PM}$$

$$(7) \quad \psi_{sq} = L_q i_{sq}$$

where: v_{sd}, v_{sq} - dq components of the stator voltage vector; i_{sd}, i_{sq} - dq components of the stator current vector; R_s - stator phase resistance; ψ_{sd}, ψ_{sq} - dq components of the stator flux vector; L_d, L_q - direct and quadrature stator

inductances; ψ_{PM} - flux established by the permanent magnets; n_p - number of pole pairs of PMSG; ω_e - the electrical angular speed of the PMSG rotor, defined as:

$$(8) \quad \omega_e = n_p \cdot \omega_m$$

The electromagnetic torque of PMSG generator is expressed as follows:

$$(9) \quad T_e = \frac{3}{2} n_p (\psi_{sd} i_{sq} - \psi_{sq} i_{sd})$$

Low-Voltage Ride-Through requirements

Voltage sags are considered as temporary decreases of the rms voltage magnitude. Voltage sags are usually caused by the faults in the power system. The voltage sags constitute the very important problem of power quality. According to the European and Polish standards, the voltage sags are defined as decreases of the voltage magnitudes between 0.9 and 0.01 per unit of the voltage rms value. In general, the voltage sags can be divided into symmetrical and unsymmetrical. The classification of possible types of the voltage sags has been presented in [2, 10].

During the voltage sags, the wind turbine system should meet the requirements relating to the connection to the AC grid. The considered LVRT requirements, obtained from typical grid code are shown in Figure 1 and 2 [2, 4].

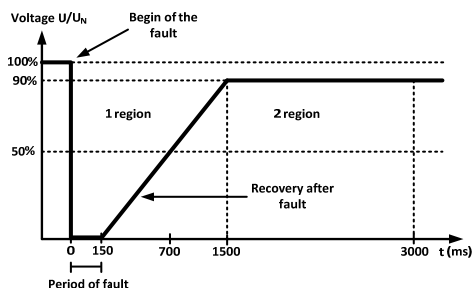


Fig.1. Voltage limit curves to allow generator disconnection

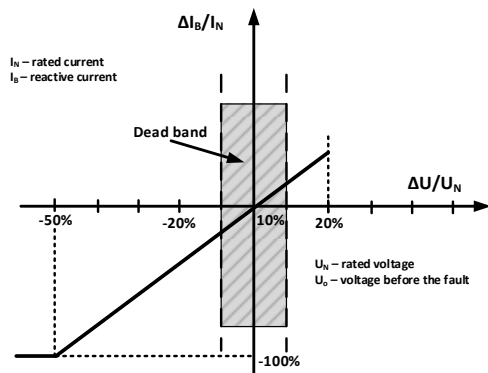


Fig.2. Characteristic of reactive current injection during voltage sags

From Figure 1, it can be observed, that when the system is operated in 1 region and when grid voltage sag occurs, the wind energy conversion system must remain connected to the grid. Whereas in case of operation in region 2, the WECS should be disconnected from the system [2, 4, 5].

In order to support the AC grid during voltage sags, the WECS must deliver to the AC grid the appropriate value of the reactive power. The average value of the reactive current delivered to the AC grid can be calculated according the characteristic presented in Figure 2 [2, 4]. The value of injection of the reactive current is dependent on the reduction of grid voltage.

Control of back-to-back converter system

The proposed control scheme for the direct-driven wind energy conversion system with PMSG has been presented in Figure 3. This scheme ensures the operation of the control system during both the normal states and the voltage sags.

For this purpose the control scheme have been divided into two switched control topologies. The first topology is concerned to the normal operation of the wind turbine system. It means, that the wind turbine operates with application of the Maximum Power Point Tracking algorithm (MPPT). This algorithm allows to obtain the maximum power at the whole range of the wind speeds.

The second control topology is applied as the special switchable technique of the control strategy with taking into account the LVRT requirements. At the application of this topology, the additional control scheme are appended to the control blocks. These additional control blocks are activated only in the case, when the voltage sags are detected by the grid fault detector. In Figure 3, the extra control blocks have been marked in dash line.

For the control of Machine Side Converter (MSC) the Rotor Field Oriented Control (RFOC) has been applied. The control scheme consists of three control loops with PI controllers: one for outer control and two for inner control.

The signal of reference angular turbine speed ω_{mopt} is established through MPPT algorithm. This algorithm allows to obtain the maximum power from the wind turbine at variable wind speeds. At the normal operations, the outer control loop is responsible for control of the turbine speed ω_m to follow the reference speed ω_{mopt} . The two inner control loops are designated for control of stator current vector components i_{sd} , i_{sq} . In the control system it is adopted, that the component i_{sd} of the stator current vector is always maintained on the zero value [1, 8]. The output signals from these controllers determine the reference components of stator voltage vector V_{sd}^* , V_{sq}^* . These reference voltages are then transformed to the $\alpha\beta$ stationary system. These voltage determine the required voltage vector for Space Vector Modulation (SVM) of MSC.

In the control of Grid Side Converter (GSC) the Vector Current Controller with Feedforward (VCCF) of negative sequence grid voltage has been applied. The main function of GSC is to delivery of the generated power to AC grid and to regulate the DC link voltage v_{dc} . The control scheme of the VCCF consists of three control loops. The outer control loop regulates the DC link voltage. The two inner control loops are designated to control of grid current vector components i_{gd} , i_{gq} . The output signals from these PI controllers are designated for the generation of the reference V_{gd}^* , V_{gq}^* and the of GSC converter voltage vector. Then these reference voltages are transformed to the $\alpha\beta$ stationary system and they represent the reference positive components of V_{ga}^+ , V_{gb}^+ grid voltage vector. During the unbalanced voltage sag, the negative sequence grid voltages V_{ga}^- , V_{gb}^- are fed-forward and added to the reference voltage. The detailed description of VCCF control method can be found in [2].

During the voltage sag, when the grid voltage drops below 90% of the rated value and the grid fault detector will detect the voltage dip, the control system is switched to the operation at the second control topology. Under a grid voltage dip, the control loop of angular rotor speed of the PMSG is disconnected. Then the control of DC-link voltage is not realized by the GSC, but by the MSC. As the voltage sag occurs, the operation of control circuits causes the reduction of generated power of the PMSG. The increase of the kinetic energy causes the raise of the mechanical angular speed of the turbine and generator.

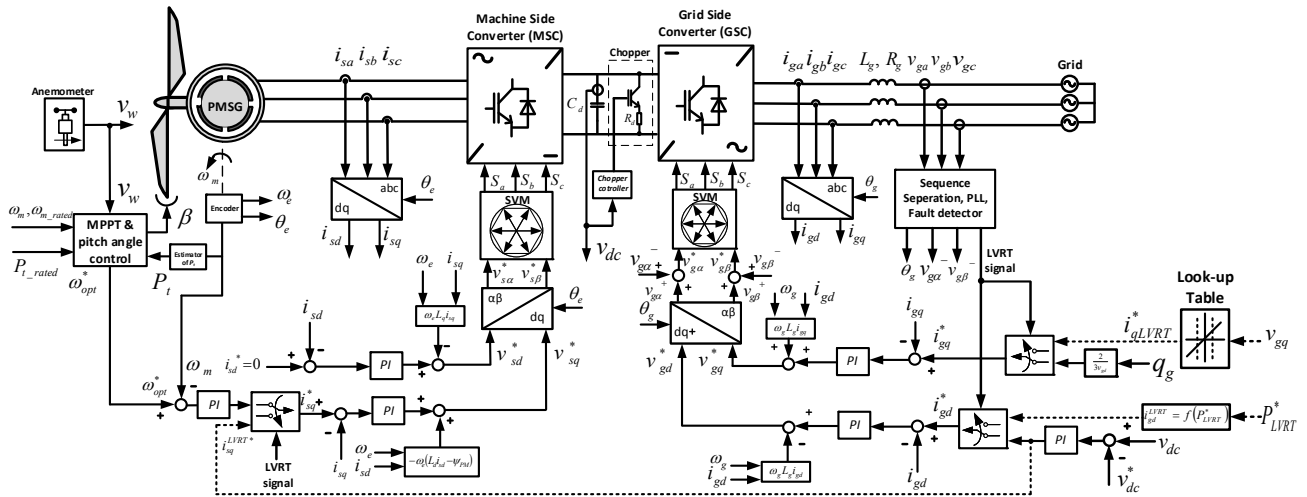


Fig.3. The scheme of variable speed wind turbine system with direct-driven PMSG generator and back-to-back converter system

In order to prevent the increase of angular rotor speed above the rated speed, the pitch angle controller should be applied.

During the activation of this control operation, the component i_{sq} of stator current vector is forced to value near zero. This means, that the electromagnetic torque of PMSG will also forced to be close to zero. This condition ensures, that the balance of the DC power between the MSC and GCS will be achieved.

During voltage dip the switching topology of the DC-link control loop is disconnected. As the same time, the considered reference instantaneous active power P_{LVRT} is set to zero in the control system. This condition causes, that the reference component i_{gd} of the grid current vector is also set to zero value [2, 5].

Despite the topology switching of the control scheme, the DC-link voltage may increase to extremely high value. This state is very dangerous for the operation of back-to-back converter system. For this reason in the control scheme, the DC bus is additionally protected by the application of the chopper with the damping resistor R_d . The unbalanced power between MSC and GSC is dissipated through the pulse controlled damping resistor.

In the control scheme it is also assumed that the reactive power is injected to the AC grid to support the grid during the voltage sags. The value of the reference reactive current component i_{gq} of the grid current vector can be calculated according to the considered LVRT requirements, which have been presented in the Figure 2.

After clearance, when the grid voltages are recovered to the nominal values, the control scheme of back-to-back converter system is switched to the topology for the normal operation.

Low voltage ride through techniques

In order to prevent the harmful effects of grid voltage dips in wind energy conversion system the three special control techniques have been used: kinetic energy storage in inertia of the wind turbine, chopper with damping resistor and pitch angle control [2, 5].

Pitch angle control

When the wind speeds or turbine rotor angular speeds exceed the rated values, then the pitch angle controller should increase the pitch angle. The increasing of pitch angle of blades results the decreasing of the power coefficient C_p of the wind turbine [1]. Consequently, the mechanical power produced by the wind turbine system will be also reduced. The block diagram of the typical pitch angle controller has been presented in Figure 4 [5, 6].

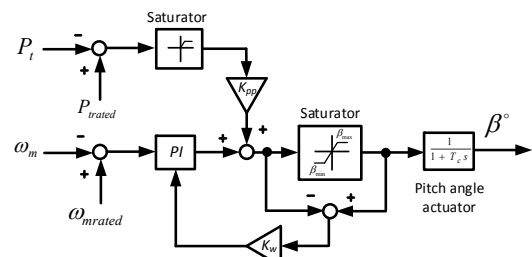


Fig.4. Wind turbine pitch angle controller

In the pitch angle controller two control loops have been applied: the main control loop of wind turbine speed and the additional control loop of wind turbine mechanical power.

In the considered control scheme it is assumed, that the reference values are equal to the rated values. In the main control loop the rated speed ω_{mrated} of wind turbine is compared with the measured turbine rotor speed ω_m . In this loop the PI controller with anti-windup system has been applied. In the additional control loop the rated turbine power P_{trated} is compared with the measured turbine power P_t . The output signals from these two control loops are added and designate the control signal of pitch angle actuator.

DC chopper

The DC chopper with damping resistor is installed in the DC bus of the MSC and GSC. The surplus power during the grid voltage sag should be dissipated by application of the damping resistor controlled through chopper [1, 2, 5]. It is assumed, that the chopper is switched on only in the case when DC-link voltage is greater than the 1.05 of the reference value V_{dcref} . Then the surplus energy is dissipated on the damping resistance R_d .

Synchronization system – DSOGI

In the control scheme of VCCF the angle θ_g is determined by the Synchronous Reference Frame - Phase Locked Loop (SRF-PLL) block [10, 11, 12]. The structure of the SRF-PLL system includes the feedback system with PI controller, tracking the phase angle of grid voltage vector.

The SRF-PLL systems have good properties and responses under grid voltage symmetry. However, during the unsymmetrical grid voltages the SRF-PLL becomes useless to determine the proper angle position of the grid voltage vector. For this reason the various synchronization techniques using the PLL have been presented in literature [1, 10, 11, 12].

The one of the proposed solutions is the Dual Second Order Generalized Integrator (DSOGI-PLL). The DSOGI-PLL has good performances in respect of the determination of proper position of the grid voltage vector in the case of the unsymmetrical grid voltages [10, 11].

The application of DSOGI-PLL guarantees the correct detection of the angle of the grid voltage vector. The operation principle of DSOGI scheme is based on the instantaneous symmetrical components theory [10]. The block scheme of SOGI has been presented in Figure 5.

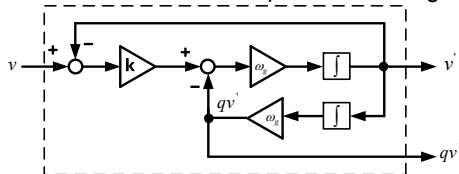


Fig.5. The scheme of SOGI

The operation of SOGI control is based on the second order transfer functions:

$$(11) \quad G_1(s) = \frac{v'}{v}(s) = \frac{k\omega_g s}{s^2 + k\omega_g s + \omega_g^2}$$

$$(12) \quad G_2(s) = \frac{qv'}{v}(s) = \frac{k\omega_g^2}{s^2 + k\omega_g s + \omega_g^2}$$

where ω_g - grid voltage angular frequency, k - damping factor. v , v' , qv' - respectively, the input signal and the two output signals: one in phase and second in quadrature with input signal.

The transfer function $G_1(s)$ operates as the band pass filter, while the $G_2(s)$ operates as low pass filter. The recommended value of coefficient for SOGI damping factor is equal to $k = \sqrt{2}$ [10]. The block scheme of DSOGI-PLL with sequence calculation is presented in Figure 6 [10].

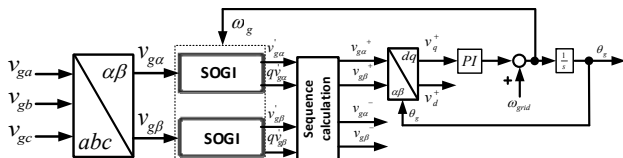


Fig.6. DSOGI PLL block diagram

Simulation Results

The simulation model of wind energy conversion system with the considered control systems has been implemented in MATLAB/Simulink. Digital simulation studies were made for the system with wind turbine data and parameters: rated power $P_T=20$ kW; blade radius $R = 4,4$ m; air density $\rho=1,225$ kg/m³ and 3-phase PMSG data and parameters: rated power $P_g=20$ kW; stator rated phase current $I_{sn}=35,1$ A; rated speed $n_n= 211$ rpm; stator resistance $R_s= 0,1764$ Ω ; stator dq -axis inductance $L_d, L_q=4,48$ mH. The simulation studies has been conducted for low power system, because the results will be compared with experimental results obtained from the laboratory test.

The obtained simulation results of considered wind energy conversion system during voltage dips are presented in Figures 7 and 8. The simulation results concerning of the behaviour of the GSC under unsymmetrical grid voltage sag have been shown in Figure 7. The three phase grid voltages v_{gabc} during the voltage sag have been presented in Figure 7a. It is assumed, that the voltage drop occurred only in phase A, and this drop of the voltage in phase A is equal to 45% of the rated grid

voltage. The considered voltage sag is starting at 0.15s, and in the 0.3s the grid voltage is starting to recover.

The waveforms of three phase grid current i_{gabc} during grid voltage sag have been presented in Figure 7b. The amplitudes of grid phase currents do not exceed the rated value of the GSC current.

During the voltage sag the control loop of the DC-link is switched to the voltage sag loop of the generator torque to reduce the active power to the zero. The waveform of the DC-link voltage v_{dc} has been shown in Figure 7c. The average value of DC-link voltage is constant at its reference value $v_{dc}=690$ V. From this Figure it can be observed, that when the grid voltage sag occurs, the DC-link voltage has been slightly increased. The proper operation of chopper can be observed. It means, that the surplus power is dissipated in the damping resistor.

In normal operation of wind turbine system, before the voltage sag, the instantaneous reactive power is set to zero. This condition allows to obtain the operation at unity power factor. This state is typical for the operation of wind turbine system. However, under the grid fault, the instantaneous active power p_g is set to zero, so there is no active power delivered to the AC grid. Then begins the support of the AC grid by injection of the reactive power. The waveforms of instantaneous active and reactive grid power p_g, q_g have been presented in Figure 7d. The oscillations of the instantaneous active and reactive power are related to the VCCF method [2].

The waveforms of grid current vector components i_{gd} and i_{gq} have been illustrated in Figure 7e. From this Figure it can be stated, that during the sag the component of grid current i_{gd} is set to the zero, which is caused by the reference value of the active power in the control scheme. Then the component of grid current i_{gq} is set to the reference value according characteristic determined LVRT requirements.

The waveforms of angular grid voltage vector position θ_g obtained from DSOGI-PLL have been illustrated in Figure 7f. From these waveforms the proper operation of DSOGI-PLL can be observed. The application of DSOGI-PLL allows to determine the proper angle of grid voltage vector even in the case of unbalanced voltage dips.

The simulation results focusing of the behaviour of the MSC during the voltage sags have been presented in Figure 8.

The angular rotor speed ω_m of PMSG and reference speed ω_{opt} obtained from MPPT algorithm have been shown in Figure 8a. From this Figure it can be noticed, that during the voltage sag, the energy storage in inertia of wind turbine system causes the increasing of angular rotor speed of PMSG and wind turbine. The waveforms of three phase stator currents i_{sabc} of PMSG have been shown in Figure 8b. The components i_{sd}, i_{sq} of stator current vector have been presented in Figure 8c. During the grid voltage sags, the both components i_{sd}, i_{sq} of the stator current vector are forced to be zero. The waveforms of power coefficient C_p and blade pitch angle β have been presented in Figure 8d and 8e. From these Figures it can be observed, that when the angular rotor speed is increased due to voltage sag, the turbine power coefficient is reduced by blade pitch angle control. In Figure 8f the control pulses of chopper with damping resistor has been shown. After clearance of the voltage sag, the control of wind energy conversion system has been returned to the normal operation with MPPT. From Figure 8a it can be observed, that the angular rotor speed of PMSM will be continuously follow the reference speed obtained from MPPT.

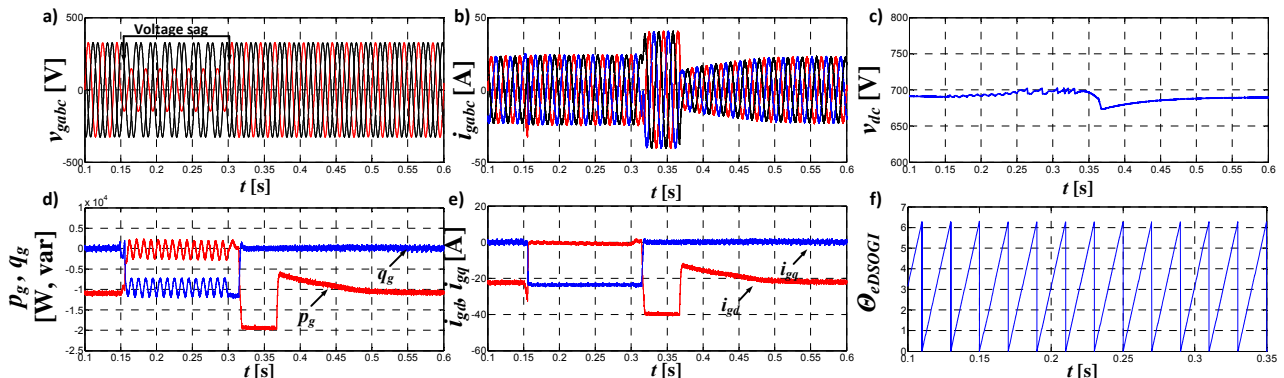


Fig.7. Simulation results of the GSC responses during grid voltage dip: a) waveforms of the three phase grid voltage v_{gabc} , b) waveforms of the three phase grid current i_{gabc} , c) waveform of the DC-link voltage v_{dc} , d) waveforms of the instantaneous active and reactive grid power p_g, q_g , e) waveforms of the grid current vector components i_{gd}, i_{gq} , f) waveform of the grid angle position θ_g .

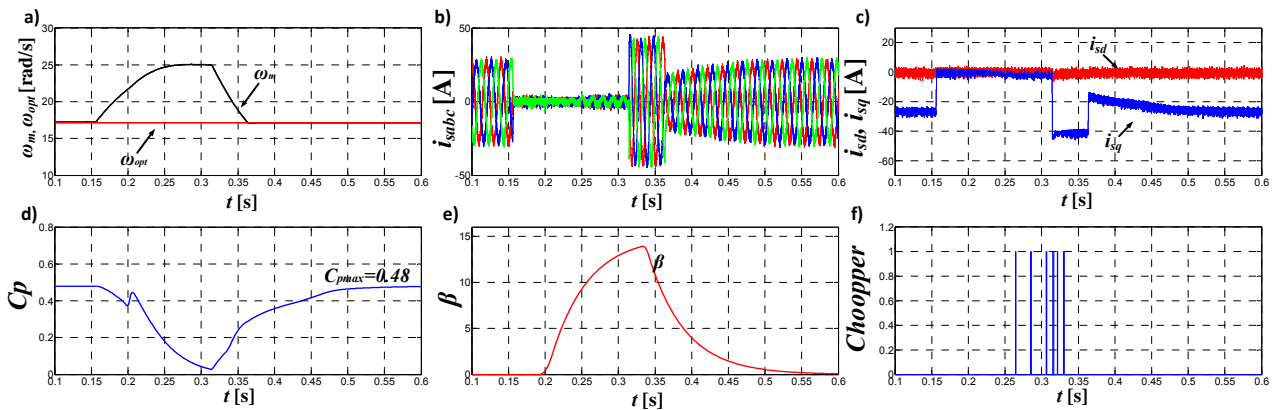


Fig.8. Simulation results of the MSC responses during grid voltage dip: a) waveforms of the reference speed ω_{opt} and measured speed ω_m of PMSG, b) waveforms of the three phase stator current of PMSG i_{sabc} , c) waveforms of the stator current vector components i_{sd}, i_{sq} , d) waveform of the power coefficient C_p ; e) waveform of the blade pitch angle β , f) waveforms of the triggering pulses of the chopper

Conclusions

In this paper the control strategy of wind energy conversion system for fulfill the LVRT requirements has been investigated. The use of the storage energy in inertia of wind turbine and pitch angle controller allows to deal with voltage dips. In order to improve the reliability and fast reaction the chopper with damping resistor has been applied in the DC link. The application of these methods allows to manage with harmful effects of LVRT.

In the synchronization system of GSC the application of DSOGI-PLL allows to obtain the proper angular voltage vector position for the balanced and unbalanced voltage dips. The simulation results confirmed that the considered control strategy has good performance during the unsymmetrical voltage dips.

Authors: Piotr Gajewski, M.Sc., Krzysztof Pieńkowski, D.Sc., Ph.D., Wrocław University of Science and Technology, Department of Electrical Machines, Drives and Measurements, ul. Wybrzeże Wyspiańskiego 27, 50-370 Wrocław
piotr.gajewski@pwr.edu.pl, krzysztof.pienkowski@pwr.edu.pl

REFERENCES

- [1] Wu B., Youngquan., Navid Z., Samir L., Power Conversion and Control of Wind Energy, John Wiley & Sons, INP., Publication, 2011.
- [2] ALepuz S., Calle A., Busquets-Monge S., Kouro S., Wu B., Use of stored energy in PMSG rotor inertia for low-voltage ride-through in back-to-back NPC converter-based wind power systems, *IEEE Transactions on Industrial Electronics*, vol. 60, no.5, may 2013, pp. 1787-1796.
- [3] Ibrahim R. Hamand M.S., Dessouky Y.G., Williams B.W., A review of recent low voltage ride-through solutions for PMSG

wind turbine, *International Symposium of Power Electronics, Electrical Drives, Automation and Motion*, 2012, pp. 265-270.

- [4] Jarzyna W., Szcześniak P., Praca generatorów elektrowni wiatrowych podczas zapadów napięcia, *Sterowanie w Energoelektronice i Napędzie Elektrycznym – SENE*, 2013.
- [5] Rizo M., Rodriguez A., Bueno E., Rodriguez F.J., Girón C., Low voltage ride-through of wind turbine based on interior Permanent Magnet Synchronous Generators sensorless vector controlled, *IEEE Energy Conversion Congress and Exposition*, Atlanta, GA, 2010, pp. 2507-2514.
- [6] Xiao-ping Y., Xian-feng D., Yan-li B., Asymmetrical voltage dip ride-through enhancement of directly driven wind turbine with permanent magnet synchronous generator, *International Conference on Sustainable Power Generation and Supply, Nanjing*, 2009, pp. 1-6.
- [7] Shen-wen L., Guang-qing B., A novel LVRT of Permanent Magnet Direct-Driven Wind Turbine, *Power and Energy Engineering Conference, Asia-Pacific*, 2011, pp. 1-4.
- [8] Gajewski P., Pieńkowski K., Advanced control of direct-driven PMSG generator in wind turbine system, *Archives of Electrical Engineering*, 2016, vol. 65, no.4, pp. 634-656.
- [9] Gajewski P., Pieńkowski K., Direct torque control and direct power control of wind turbine system with PMSG, *Przegląd Elektrotechniczny*, R. 92, no.10, 2016, pp 249-253.
- [10] Bobrowska-Rafał M., Grid synchronization and control of three-level three-phase grid-connected converters based on symmetrical components extraction during voltage dips, *Ph.D Thesis, Electrical Dep., Warsaw University of Technology*, (2013).
- [11] Blaabjerg F., Teodorescu R., Liserre M., Timbus A.V., Overview of control of grid synchronization for disturbed power generation system, *IEEE Transactions of Industrial Electronics*, vol. 53, no.5, October 2006, pp. 1398-1409.
- [12] Lipnicki P., Przegląd metod PLL do synchronizacji z siecią przekształtników energoelektrycznych, *IAGPOŚ*, 2003, pp. 5-8.